Scanning Electrochemical Microscopy. 15. Improvements in Imaging via Tip-Position Modulation and Lock-in Detection

David O. Wipf and Allen J. Bard*

Department of Chemistry and Biochemistry, The University of Texas at Austin, Austin, Texas 78712

The use of small amplitude tip-position modulation (TPM) in combination with lock-in detection of the modulated current signal greatly improves the sensitivity and image resolution of the scanning electrochemical microscope and provides a method of distinguishing between conductive and insulating areas on the substrate surface being examined. The experimental in-phase current versus distance behavior is characterized for insulating and conducting surfaces for various modulation amplitudes and frequencies. A simple derivative model of the dc response is adequate to derive the in-phase TPM response at conductors; the insulator response does not conform to the theory and is, in fact, more sensitive than predicted. Demonstration images of an interdigitated array electrode using the dc and in-phase TPM signal are compared. The in-phase TPM image is found to be superior for imaging because of its improved sensitivity to insulating surfaces and its bipolar response over insulators and conductors.

INTRODUCTION

In this paper we describe tip-position modulation scanning electrochemical microscopy (TPM SECM), a new mode of operation of the scanning electrochemical microscope (SECM). SECM is a scanned-probe microscopy that is used to study interfaces immersed in electrolyte solution.[1-3] In the feedback mode of the SECM, an ultramicroelectrode tip is used to generate a localized concentration of the oxidized or reduced form of a mediator species. Perturbations in the faradaic current from the mediator electrolysis are used to provide information about the surface topography and electronic conductivity of the substrate as the tip is rastered across the sample surface. TPM SECM is a modification of the basic feedback mode method in which the tip position (i.e., the tip–surface distance) is modulated with a small-amplitude sinusoidal motion normal (z direction) to the sample surface. The modulated current is then used as the imaging signal.

Feedback SECM is a versatile technique in that it can be used to image both insulating and electronically conducting substrates. Information about the conductive nature of the substrate is obtained by comparison of the tip current during imaging, i_T, when the tip is within a few tip radii from the substrate surface, with the current when the tip is far from the substrate, $i_{T,\infty}$. Conductive substrates give a positive feedback ($i_T > i_{T,\infty}$); insulators, negative feedback ($i_T < i_{T,\infty}$). However, if $i_{T,\infty}$ is not known, one cannot distinguish a drop in current caused by a topographic change in a conductor (e.g., an increase in the tip–substrate distance) with movement into an insulating region. As shown below, TPM provides such a distinction, without knowledge of $i_{T,\infty}$. This case can arise, for example, when one simply wants to use the SECM to image a substrate without taking an approach (i_T vs distance) curve or when an irreversible reaction (e.g., oxygen reduction) occurs at the tip in addition to the desired mediator reduction reaction. Because of the chemical specificity obtained by use of a mediator, SECM can be used to image variations in chemical, electrochemical, and enzyme activity (reaction-rate imaging) at resolutions of better than 1 μm.[1,4-6] Image resolution is improved with smaller tips, and under ideal conditions, tips of 0.1-μm radius and smaller have been used for SECM.[7,8] However, use of smaller tips leads to experimental difficulty due to signal-to-noise reduction because of the smaller imaging current. In addition, the SECM imaging signal is not ideal since it is present on a large dc offset, i.e., $i_{T,\infty}$.[9]

The TPM SECM technique alleviates these difficulties since the modulation process shifts the signal from dc frequencies to the modulation frequency, thus removing the dc offset and the associated low-frequency noise sources (i.e., drift).[10] In addition, use of phase-sensitive lock-in amplification to measure the ac signal reduces noise further by limiting the measurement bandwidth. Imaging with the TPM SECM is demonstrated and is shown to produce superior images compared to simple feedback SECM.

The principle of TPM is shown schematically in Figure 1A. The tip is moved sinusoidally in the z direction so that its distance from the substrate is modulated by $\pm\delta/2 \sin 2\pi f_m t$ about its average distance, d. This modulation causes a modulation in the tip current at the same frequency, as shown in Figure 1B. Since a positive change in z (movement away from the surface) causes a decrease in the tip current over a conductor but an increase over an insulator, i_T(conductor) and i_T(insulator) are 180° out-of-phase. Thus by detecting the in-phase component of the modulated current with a lock-in amplifier, one can identify the conductive nature of the surface, as well as take advantage of the noise reduction available by this mode of detection.

EXPERIMENTAL SECTION

Reagents. $Ru(NH_3)_6Cl_3$ (Strem Chemicals, Newburyport, MA) was used as received. The electrolyte solution for all experiments was a pH 4.0 phosphate–citrate (McIlvaine) buffer made to 0.5 M ionic strength with KCl.

Electrodes. Ultramicroelectrode tips were prepared by sealing either 2-μm-diameter (Goodfellow Metals, Cambridge UK) or 8-μm-diameter carbon fiber wires (AVCARB CF125G type F84, Textron Specialty, Lowell, MA) into Pyrex tubes. Disk-shaped electrodes were exposed by grinding the sealed tube end with emery paper and then polishing with diamond and alumina polish and finishing with 0.05-μm alumina on felt. The glass insulating sheath was ground down with 600-grit emery paper to form a tip in the shape of a truncated cone. This step is essential to

(1) Bard, A. J.; Fan, F.-R.; Pierce, D. T.; Unwin, P. R.; Wipf, D. O.; Zhou, F. *Science* **1991**, *254*, 68.
(2) Bard, A. J.; Denuault, G.; Lee, C.; Mandler, D.; Wipf, D. O. *Acc. Chem. Res.* **1990**, *23*, 357.
(3) Engstrom, R. C.; Pharr, C. M. *Anal. Chem.* **1989**, *61*, 1099A.
(4) Wipf, D. O.; Bard, A. J. *J. Electrochem. Soc.* **1991**, *138*, L4.
(5) Wipf, D. O.; Bard, A. J. *J. Electrochem. Soc.* **1991**, *138*, 469.
(6) Pierce, D. T.; Unwin, P. R.; Bard, A. J. *Anal. Chem.*, submitted for publication.
(7) Lee, C.; Miller, C. J.; Bard, A. J. *Anal. Chem.* **1991**, *63*, 78.
(8) Fan, F-R.; Bard, A. J., unpublished results.
(9) Kwak, J.; Bard, A. J. *Anal. Chem.* **1989**, *61*, 1221.
(10) Hieftje, G. M. *Anal. Chem.* **1972**, *44*, 81A.

0003-2700/92/0364-1362$03.00/0

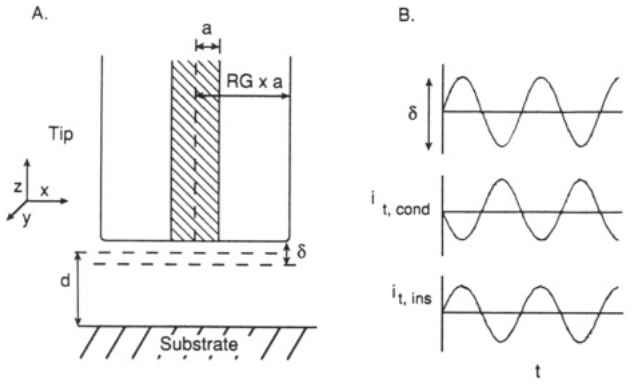

Figure 1. (A) Schematic diagram of the tip-position modulation experiment. (B) Idealized representation of the tip position and currents observed over insulating and conducting substrates with time.

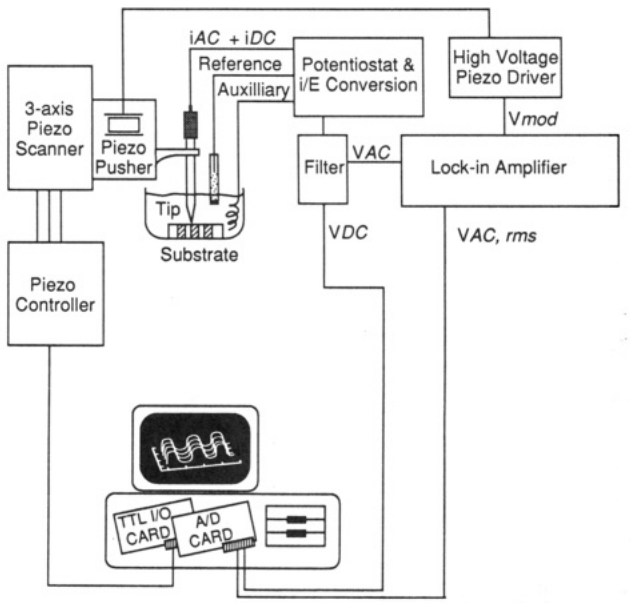

Figure 2. Block diagram of the tip-position modulation SECM.

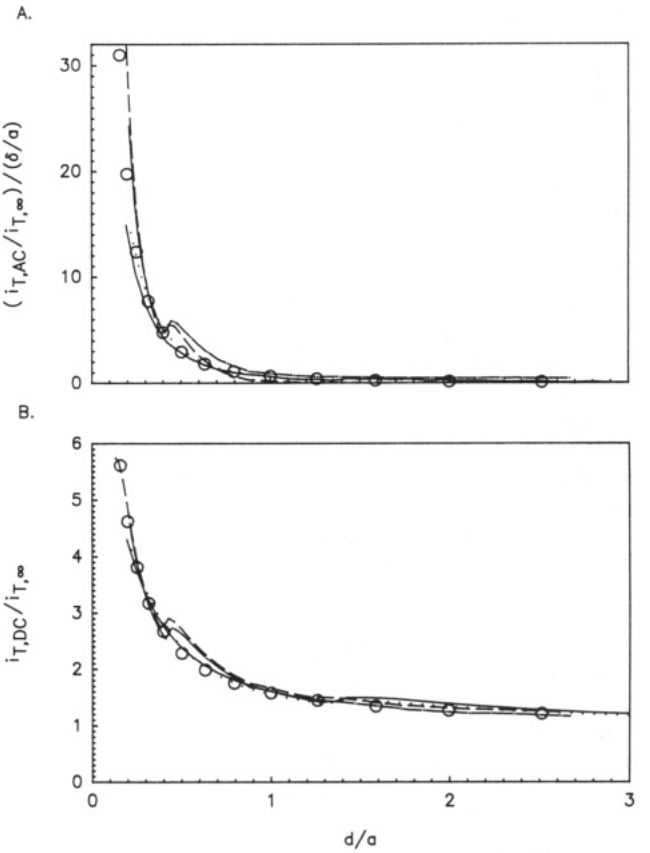

Figure 3. Experimental and theoretical SECM and TPM SECM current vs distance plots at a conductive Au substrate. Mediator is 2.0 mM $Ru(NH_3)_6^{3+}$ in pH 4.0 buffer. Tip electrodes are 1-μm radius Pt, RG = 5; or 4-μm-radius C-fiber, RG = 10. (A) In-phase modulated current; (O) eq 2; (—) a = 1, δ/a = 0.01, f_m = 100 Hz, tip scan rate = 0.05 μm/s; (•••) a = 1, δ/a = 0.05, f_m = 100 Hz, tip scan rate = 0.05 μm/s; (- - -) a = 4, δ/a = 0.025, f_m = 100 Hz, tip scan rate = 0.1 μm/s; (- • -) a = 4, δ/a = 0.125, f_m = 40 Hz, tip scan rate = 0.1 μm/s. The small deviation in the experimental data at d/a = 0.5 is an artifact due to the clamping action of the coarse piezo positioners. (B) dc (O) eq 1; see A for key to data.

experimental success; otherwise, the inevitable deviation of the tip surface and substrate from parallel approach will allow the sheath to contact the substrate and thus prevent a close tip–substrate spacing. The ratio (RG) of the radius of the glass sheath to the radius of the exposed disk was from 5 to 10. Substrates used were evaporated gold (200-nm Au on 10-nm Cr on glass), an interdigitated electrode array (IDA, 3-μm-wide Pt bands separated by 5-μm-wide SiO_2 insulator, a gift from Melani Sullivan, University of North Carolina at Chapel Hill), and glass microscope slides. The tip electrode was polished with 0.05-μm alumina on felt (Buehler, Ltd., Lake Bluff, IL) before each experimental run. The substrates were used after an ethanol and distilled water rinse. Potentials were recorded versus a Ag/AgCl reference electrode in 3 M KCl or a Ag wire QRE. The auxiliary electrode was Pt gauze or wire.

Experimental Apparatus. The apparatus for the tip-modulated SECM experiment is similar to that described previously.[5] Several additional components have been added to perform the ac experiment (Figure 2). Modulation of the tip position was achieved by mounting the tip onto a spring-loaded linear translation stage (Model 421-OMA, Newport Corp., Fountain Valley, CA) driven by a piezoelectric pusher (PZT-30, Burleigh Instruments, Inc., Fishers, NY) with a nominal displacement of 5 nm/V. The modulation voltage, V_m, for the pusher was derived from the sine-wave reference oscillator output of a lock-in amplifier (Model 5206 or 5210, two-phase lock-in amplifier, EG&G PAR, Princeton, NJ) and amplified to the desired value by a high-voltage dc amplifier (PZ-70, Burleigh Instruments).

Experimental Procedure. For the experiments described here, the SECM response is assumed to be solely limited by diffusion control. The tip potential in all cases was set to a value sufficiently negative that the mediator reduction was diffusion-controlled.[5] The conductive substrates were not externally biased. However, for these experimental conditions, the substrate rest potential is sufficiently positive of the mediator redox potential that the substrate reaction below the tip is diffusion-limited. The tip-modulated SECM experiments were similar to the conventional experiment, but in this case the tip-current is composed of the normal dc component and an ac component induced by the piezo motion. The dc response was measured after current-to-voltage conversion and filtering at 15 Hz to remove the ac component (Figure 2). The modulation signal was measured with the lock-in amplifier to generate the phase-resolved root mean square (rms) ac response. For all the experiments, the dc and ac signals were acquired simultaneously so that the data could be directly compared. Other details concerning tip positioning and scanning have been described.[11]

RESULTS AND DISCUSSION

TPM SECM at Conducting Substrates. Experimental in-phase TPM and dc SECM responses versus tip–substrate separation, d, at a conductive substrate are shown in Figures 3A and 3B. These data were acquired for various values of the peak-to-peak tip-distance modulation, δ, electrode radius, a, and modulation frequency, f_m. The distance axis is normalized by dividing d by the radius to give d/a. The tip current, $i_{T,DC}$, for the dc response in Figure 3B is normalized

(11) Kwak, J.; Bard, A. J. *Anal. Chem.* **1989**, *61*, 1794.

by the i_T value measured at a large d value, $i_{T,\infty}$. The rms in-phase modulated tip current, $i_{T,AC}$, is normalized by division by $i_{T,\infty}$ and by the ratio of δ_{rms}/a, where δ_{rms} is the rms value of the peak-to-peak modulation distance.

For sufficiently small δ, the in-phase TPM signal can be considered to be the derivative of the dc conductor response. A good approximation of the theoretical dc current–distance response is given by[12]

$$i_{T,DC}/i_{T,\infty} = 0.68 + 0.78377/L + 0.3315 \exp(-1.0672/L) \quad (1)$$

where $L = d/a$. The derivative is

$$d(i_{T,DC}/i_{T,\infty})/dL = (-0.78377 + 0.3538 \exp(-1.0672/L))/L^2 \quad (2)$$

The experimental dc data can be fit to eq 1 to determine $i_{T,\infty}$ and the absolute tip–substrate distance for the TPM experiment (Figure 3B). This allows the experimental TPM data to be compared to eq 2 with no adjustable parameters. As is seen, the agreement is excellent. Note that the derivative has been inverted to match the polarity of the experimental data.

The tip-modulation frequency in these experiments is limited to a small range. However, Figure 3 shows that data taken at f_m values of 40 and 100 Hz are essentially identical. The lower limit for modulation frequency is governed by the time scale of the experiment. Frequencies lower than 40 Hz require measurement times that are too long to be usable in an imaging experiment and would also interfere with the dc signal. We also find the mechanical response of the tip holder limits our experiments to an upper frequency of about 160 Hz.

The effect of the tip-modulation distance, δ, was investigated by varying the dimensionless ratio of δ/a over a range of 0.01 to 1.0. Over this range, the TPM signal was directly proportional to this ratio. However large δ/a values lead to experimental difficulties. The closest approach of the tip to the substrate surface is $\delta/2$, limiting sensitivity. A further difficulty is that, at sufficiently large δ/a values, the dc signal is perturbed by the tip modulation. Because the tip current is not a linear function of distance (eq 1), the distance modulation signal is rectified to supply an additional dc current. This is analogous to faradaic rectification found in electrochemical experiments when an ac modulation is applied under conditions where the i–E characteristic is nonlinear. This effect can be calculated by integrating the modulation current over a modulation cycle. The calculation shows that, for sinusoidal modulation, the dc current is roughly 10% larger than expected when the ratio of δ/a is greater than $0.4d/a$. Thus, as a rule of thumb, only d values greater than 2.5δ should be used.

Comparison of the TPM and dc signals show that there are a number of advantages in the use of the TPM signal. The first is that the TPM signal has an absolute baseline of zero at large d, in contrast to the baseline of $i_{T,\infty}$ for the dc data. Also the TPM signal is more sensitive to d at close distances. Both of these characteristics tend to make the TPM signal a more precise and accurate signal for imaging with the SECM.

TPM at Insulating Substrates. Experimental in-phase TPM and dc SECM responses versus tip–substrate separation, d, at an insulating substrate are shown in Figures 4A and 4B. These data were acquired for various values of tip-modulation distance, δ, electrode radius, a, and modulation frequency, f_m. As for the conductor case, the TPM and dc signals were acquired simultaneously and are shown in the same dimensionless form. An approximation of the theoretical current

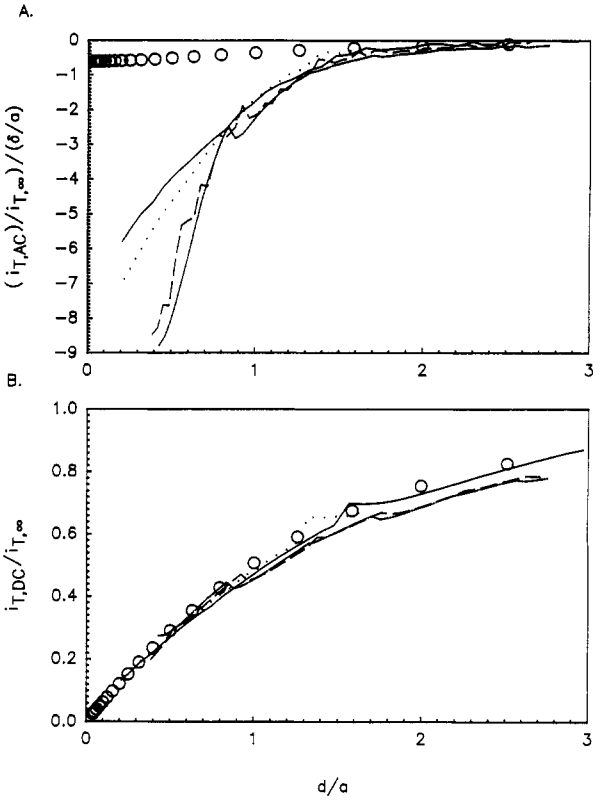

Figure 4. Experimental and theoretical SECM and TPM SECM current vs distance plots at an insulating glass substrate. Mediator is 2.0 mM $Ru(NH_3)_6^{3+}$ in pH 4.0 buffer. Tip electrodes are 1-μm-radius Pt, RG = 5; or 4-μm-radius C-fiber, RG = 10. (A) In-phase modulated current; (O) eq 4; (—) a = 1, δ/a = 0.02, f_m = 100 Hz, tip scan rate = 0.05 μm/s; (···) a = 1, δ/a = 0.05, f_m = 150 Hz, tip scan rate = 0.05 μm/s; (- - -) a = 4, δ/a = 0.0125, f_m = 40 Hz, tip scan rate = 0.1 μm/s; (- · -) a = 4, δ/a = 0.125, f_m = 100 Hz, tip scan rate = 0.1 μm/s; (B) (O) eq 3; see A for key to data.

vs distance behavior for the dc signal is given by eq 3.[12]

$$i_{T,DC}/i_{T,\infty} = 1/\{0.15 + 1.5385/L + 0.58 \exp(-1.14/L) + 0.0908 \exp[(L - 6.3)/1.017L]\} \quad (3)$$

Equation 4, the predicted TPM response, is the derivative of eq 3.

$$d(i_{T,DC}/i_{T,\infty})/dL = \{1.5385 - 0.6612 \exp(-1.14/L) - 0.56249 \exp[(L - 6.3)/1.017L]\}/\{(0.15 + 1.5385/L + 0.58 \exp(-1.14/L) + 0.0908 \exp[(L - 6.3)/1.017L])L\}^2 \quad (4)$$

Equation 3 was used to fit the experimental data to estimate $i_{T,\infty}$ and d. Note that eq 3 is only strictly valid for an SECM tip with an embedded disk geometry such that the ratio of the radius of the insulating sheath around the electrode to the electrode itself is 10. The dc SECM insulator response is sensitive to this ratio (RG), and larger ratios decrease the tip current.[9] In contrast, the dc SECM conductor response is insensitive to the RG value.

The dc data shown in Figure 4B fit to eq 3 quite well, although two of the experimental current–distance curves are for an electrode with an RG value of about 5 (a = 1.0 μm). The use of eq 3 to fit this data will cause the absolute tip–substrate separation calculated from these data to be too large by about 0.2 d/a units.[9] Despite this error, the general agreement between the theory and dc experiment is good. However, the derivative of the dc current does not agree with the TPM data (Figure 4A). The curves from a tip with a =

(12) Mirkin, M. V.; Fan, F.-R.; Bard, A. J. *J. Electroanal. Chem. Interfacial Electrochem.*, in press.

1 μm and RC = 5 are different from the curves for a tip with a = 4 μm and RG = 10, and both curves show a much larger response than that predicted from eq 4.

The good agreement for the TPM signal and the dc derivative at the conductor substrate and the poor agreement at the insulator substrate reflect the different nature of the dc SECM feedback signal from these two types of surface. At a conductor, the feedback signal is predominantly due to the recycling of the mediator in the tip–substrate gap. This leads to an approximately linear concentration gradient between the tip and substrate. At an insulator, the SECM feedback current decreases because of physical blockage of the diffusion path of the mediator molecule by the presence of the insulating surface. As such, the signal is strongly dependent on the geometry of the tip, particularly the ratio RG. As a result, the concentration gradient between the tip and substrate is not linear and it extends out from the tip electrode to the edge of the tip insulator.[9] Because of the extended diffusional field and the restricted geometry, the time for the dc SECM insulator response to reach a steady state is much longer than that for the conductor response,[13-15] and this is a possible reason for the difference in the response. The TPM current vs distance curves in Figure 4A are independent of f_m over the range of 40–150 Hz. This suggests that lower frequencies would be required to reach steady state.

The larger TPM insulator response is probably not seriously affected by convection effects. In effect, the tip modulation can act as a tiny pump to replenish the solution in the tip–substrate gap. Although we have no direct evidence against this, two factors suggest that convective effects are minimal. In Figure 4A the modulation amplitude was varied by factors of 2.5 and 10 for the two electrodes used; however, the response, after scaling for the modulation amplitude, was not changed. A second point is the different response when the electrode RG value was varied. The response for the electrode with RG = 5 was smaller than that for the RG = 10 electrode. We expect from theory that smaller RG values lead to shorter times to steady state and thus ac signals from tips with smaller RG values should be closer to the current predicted by eq 4.

Although the TPM SECM signal at insulators cannot, as yet, be described theoretically, the deviations from the predicted behavior lead to significant improvements in sensitivity. Moreover, the magnitude of the TPM signal increases with decreasing tip–substrate distance from a zero baseline while the dc signal decreases, again improving sensitivity and precision. Finally, note that the TPM signals at insulators and conductors are of different sign (bipolar), as opposed to the unipolar signal with dc SECM, providing unambiguous detection of the state of the substrate surface.

Imaging with the TPM SECM. Figure 5 shows several line scans over the surface of an interdigitated array (IDA) electrode at different tip–substrate distances. These data were acquired under conditions similar to those in Figures 3 and 4 and show the TPM and dc responses as the tip is scanned parallel to the surface of the IDA electrode. The IDA consists of 3-μm-wide bands of Pt spaced by 5 μm of SiO_2 and so presents alternately conducting and insulating behavior as the tip is scanned across the surface in a direction nearly perpendicular to the band's long axis. Note that with the 1-μm tip used here, the scan resolution causes the observed band structure to be somewhat rounded. As expected, the TPM response of the line scan is bipolar and rapidly falls off with increasing distance. This contrasts with the dc signal, which is present on top of the $i_{T,\infty}$ level and has a more gradual

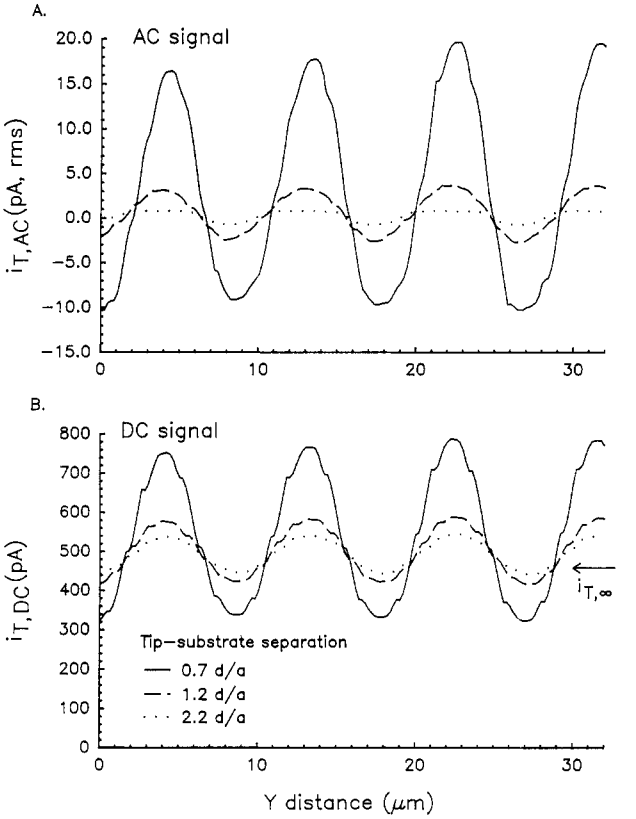

Figure 5. Line scans at various distances with TPM SECM in-phase current and SECM at the IDA electrode. Conditions: mediator, 1.5 mM $Ru(NH_3)_6^{3+}$ in pH 4.0 buffer, tip electrode, 1-μm-radius Pt; f_m = 160 Hz, δ/a = 0.1; scan speed, 2 μm/s. (A) TPM SECM response; (B) dc SECM response.

decrease. Another important distinction is the increased sensitivity in the insulator region. This is especially noticeable at larger tip–substrate separations, when the dc insulator signal is nearly swamped by the larger conductor signal. A common problem in both in-phase TPM and dc SECM is the difficulty in imaging insulating regions adjacent to conducting regions. Even when the tip is completely over the insulator the mediator species can provide some positive feedback by diffusion from the disk to the conductor edge making the observed insulator response more positive and obscuring insulator features. The application of image processing techniques, which decrease diffusional effects on SECM images,[16] should prove equally useful in TPM SECM in such circumstances.

Images of a portion of the IDA electrode acquired with dc and TPM SECM are shown in Figure 6. The band structures observed in the upper left of the image are the Pt bands with the remainder of the image the insulating SiO_2 substrate. Figure 6A is the image acquired with the dc signal while Figures 6B and 6C are TPM images. Here we see that the images acquired with the TPM signal are significantly more detailed than the dc image. In particular, note the improved detail in the insulating region of the image, due to the better sensitivity of the TPM signal at insulators. Figures 6A and 6B are plotted as gray scale, with more positive current shown as a lighter shade. However, this representation is somewhat confusing, since the insulating signal is presented with the darkest portions representing protrusions. Thus, the apparent crater-like features seen in the TPM image are actually bumps. The dc image shows the same dark spots, although these are difficult to see due to its poorer insulating sensitivity.

(13) Bard, A. J.; Denuault, G.; Friesner, R. A.; Dornblaser, B. C.; Tuckerman, L. S. *Anal. Chem.* **1991**, *63*, 1282.
(14) Unwin, P. R.; Bard, A. J. *J. Phys. Chem.* **1991**, *95*, 7814.
(15) Mirkin, M. V.; Bard, A. J. *J. Electroanal. Chem. Interfacial Electrochem.* **1992**, *323*, 29.
(16) Lee, C.; Wipf, D. O.; Bard, A. J.; Bartels, K.; Bovik, A. C. *Anal. Chem.* **1991**, *63*, 2442.

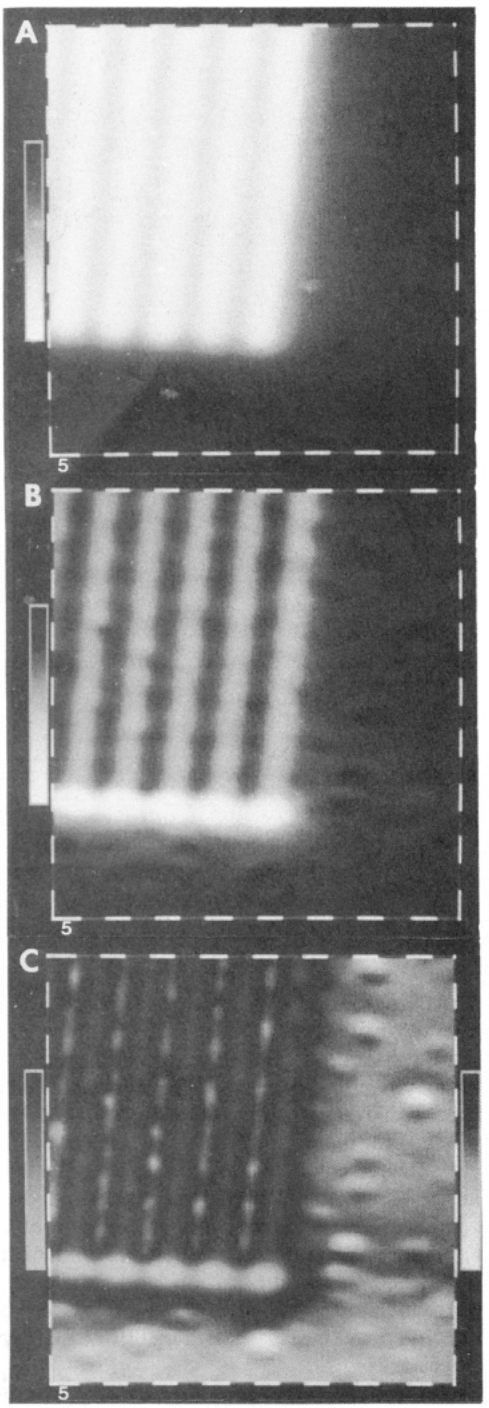

Figure 6. TPM and dc SECM images of a 80-μm × 80-μm portion of the IDA substrate. Conditions: mediator, 1.5 mM $Ru(NH_3)_6^{3+}$ in pH 4.0 buffer; tip electrode, 1-μm-radius Pt; $d \approx 0.9$ μm; $f_m = 160$ Hz, $\delta/a = 0.1$; scan speed, 10 μm/s. (A) SECM image, scale is 200–850 pA, $i_{T,\infty} = 470$ pA. (B) TPM SECM image, scale −7 to 15 pA_{rms}. (C) Absolute value TPM SECM image, left scale = 0–15; right scale = 0–7 pA_{rms}.

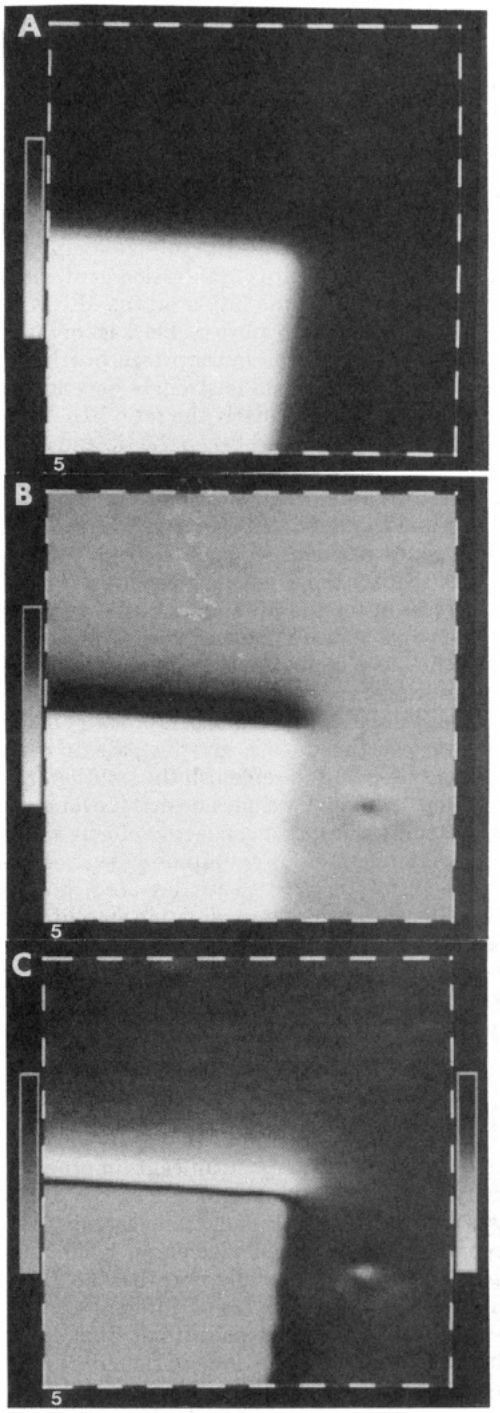

Figure 7. TPM and dc SECM images of a 80-μm × 80-μm portion of an auxilliary electrode pad on the IDA substrate. Conditions: mediator, 1.5 mM $Ru(NH_3)_6^{3+}$ in pH 4.0 buffer; tip electrode, 1-μm-radius Pt; $d \approx 0.9$ μm; $f_m = 160$ Hz, $\delta/a = 0.1$; scan speed, 10 μm/s. (A) SECM image, scale is 250–850 pA, $i_{T,\infty} = 470$ pA. (B) TPM SECM image, scale −15 to 6 pA_{rms}. (C) Absolute value TPM SECM image, left scale = 0–6; right scale = 0–15 pA_{rms}.

A more faithful representation of the image topography can be made by using the absolute value of the TPM in-phase current with separate gray or color scales for the insulating and conducting regions as is shown in Figure 6C. The features in the insulating region are now conventionally shown and are probably small dust particles on the surface of the substrate.

The enhanced distance sensitivity of the TPM signal is seen by the large currents observed at the tips of the conducting bands. The ends of the bands evidently protrude slightly above the rest of the band causing an increased signal in the dc image but an even greater signal increase with the TPM image. Thus, the apparent topographic image will be distorted by the nonlinearity of in-phase TPM current, and due care must be taken in the interpretation of such features. Alternatively, one can use a calibration curve to convert the TPM currents to actual distances. Note the advantage of SECM over optical microscopy in providing 3D (vs 2D) images.

Another image of the IDA electrode is shown in Figure 7. In this case the dc SECM and TPM SECM images show the corner of a rectangular Pt auxilliary electrode pad on the SiO_2 substrate. Figure 7A is the image acquired with the dc

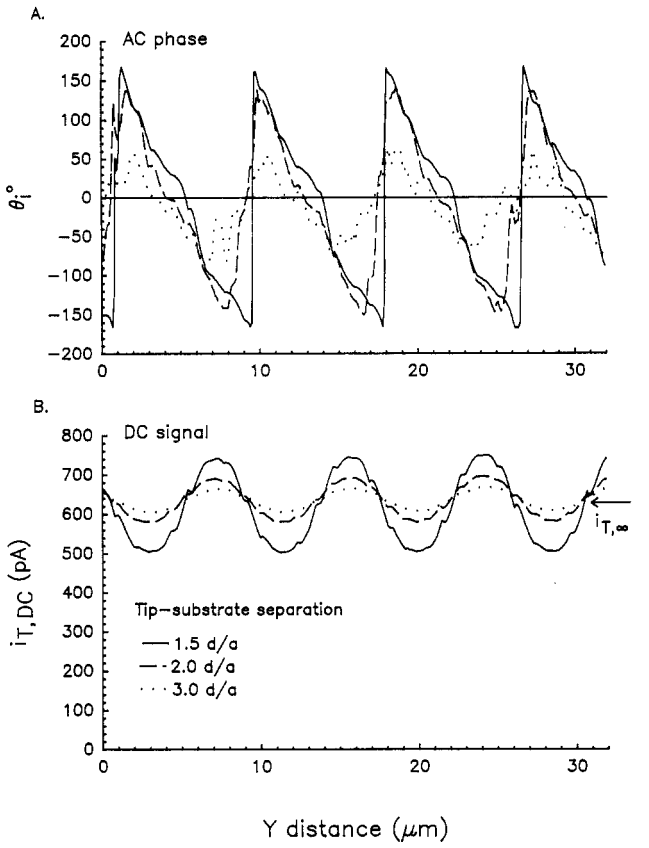

Figure 8. Line scans at various distances with TPM SECM current phase θ_i and dc SECM at the IDA electrode. Conditions: mediator, 2.0 mM $Ru(NH_3)_6^{3+}$ in pH 4.0 buffer; tip electrode, 1-μm-radius Pt; f_m = 100 Hz, δ/a = 0.1; scan speed, 1 μm/s. (A) TPM SECM response; (B) dc SECM response.

signal while Figures 7B and 7C are ac images. Again we see that the TPM images are significantly more detailed than the dc image. An interesting feature is the large negative signal along the top of the pad. This would seem to indicate the presence of a ridge of insulating material running along the top of the pad.

Phase Images. The two-channel lock-in amplifier used for this work can provide other imaging signals in addition to the in-phase current used above. A useful signal is the phase of the modulated current, θ_i. Figure 8 shows the dc signal and θ_i for line scans at different distances over the IDA electrode. The shape of the θ_i signal shown is unusual and requires some explanation. As expected from the in-phase results, the insulator and conductor responses are 180° out of phase. For these data the lock-in amplifier phase was arbitrarily advanced by 90° so that the conductor signal was maximized at −90° and the insulator signal maximized at +90°. Note that the signal is not inverted here as it is for the in-phase data. An unfortunate aspect of the θ_i signal is that, instead of θ_i smoothly varying from +90° to −90°, the lock-in amplifier has a discontinuity at ±180°. Despite this, the θ_i signal has the interesting property of being relatively insensitive to the tip–substrate separation. The effect of larger separations is to decrease the signal-to-noise of the response, rather than the magnitude. Thus, θ_i is insensitive to sample topography but is sensitive to the substrate conductivity, whereas the dc and in-phase TPM response are sensitive to both. This property would be useful for applications in which the state of the surface must be distinguished. For example, we are using this signal in the construction of a closed-loop piezo feedback control circuit to scan the tip in a constant current mode over a mixed insulator–conductor surface. Over a conductor, the dc tip current is maintained, through feedback control of the tip height, at a constant current larger than $i_{T,\infty}$. However, as the tip scans over an insulating region, the polarity change in θ_i acts as a switch to invert the direction of the feedback control signal so that the tip current can be maintained at a second control current. The use of two control currents is essential, because the dc current over an insulator is never higher than $i_{T,\infty}$ and the dc current over a conductor is larger than $i_{T,\infty}$.

CONCLUSIONS

The tip-position modulation technique described here significantly improves the information content and sensitivity of the SECM technique. We have empirically examined the nature of the in-phase ac current–distance behavior for insulating and conducting substrates as a function of modulation amplitude, frequency, and tip size. The in-phase TPM response at conducting surfaces can be modelled simply as the derivative of the steady-state dc behavior, but the response at insulating surfaces is more complex and requires further theoretical modeling. These experiments show that the in-phase TPM response has improved properties over the dc response in several respects, most notably the bipolar response for insulating and conducting surfaces and the increased sensitivity of the signal to the tip–substrate separation.

SECM images acquired with the in-phase TPM signal show superior image definition as a result of the increased sensitivity to insulating material. The modifications required to convert a dc SECM to TPM capability are minor and the modified instrument gains the capability to acquire dc and TPM data simultaneously. In addition, we anticipate other types of TPM experiments in which the modulation of the tip is in the plane of the scan direction rather than perpendicular to it. Such a modulation could improve the lateral resolution of the image, just as the vertical resolution is enhanced here.

The best resolution reported with the SECM technique is at a tip with a 0.1-μm radius.[7] To improve the resolution further requires the use of smaller tips and use of a constant current feedback mode, such as used by the STM,[17] to maintain a close tip–substrate separation. Preliminary work has demonstrated that smaller tips and constant-current imaging is possible;[8,18] however, for surfaces containing both insulating and conducting regions, constant-current imaging is difficult since the feedback controller requires information about the nature of the surface. We have shown that the tip-modulated signal can give an unambiguous indication of whether a surface is insulating or conducting. Thus, the in-phase or θ_i signal in combination with the dc signal can be used to provide constant-current imaging at mixed insulating and conducting substrates.[18]

ACKNOWLEDGMENT

The support of this research by the Robert A. Welch Foundation is gratefully acknowledged.

RECEIVED for review December 10, 1991. Accepted April 3, 1992.

Registry No. $Ru(NH_3)_6^{3+}$, 18943-33-4; Au, 7440-57-5; Pt, 7440-06-4; SiO_2, 7631-86-9.

(17) Binnig, G.; Rohrer, H. *Helv. Phys. Acta* **1982**, *55*, 726.
(18) Wipf, D. O.; Bard, A. J., unpublished results.